Aqueous Peptide-TiO_2 Interfaces: Iso-energetic Binding *via* either Entropically- or Enthalpically-driven Mechanisms

Anas M. Sultan,[1,#] Zayd C. Westcott,[2,#] Zak E. Hughes,[1] J. Pablo Palafox-Hernandez,[1] Tristan Giesa,[3] Valeria Puddu,[2] Markus J. Buehler,[3] Carole C. Perry,[2,] and Tiffany R. Walsh[1,*]*

[1]Institute for Frontier Materials, Deakin University, Geelong, Victoria 3216, Australia, [2]Interdisciplinary Biomedical Research Centre, School of Science and Technology, Nottingham Trent University, Clifton Lane, Nottingham, NG11 8NS, U.K., [3]Laboratory for Atomistic and Molecular Mechanics (LAMM), Department of Civil and Environmental Engineering, Massachusetts Institute of Technology, 77 Massachusetts Ave, Cambridge, MA 02139, USA.

[#]These authors contributed equally

RECEIVED DATE (to be automatically inserted after your manuscript is accepted if required according to the journal that you are submitting your paper to)

*To whom correspondence should be addressed:

CCP: email: carole.perry@ntu.ac.uk
TRW: email: tiffany.walsh@deakin.edu.au

Abstract

A major barrier to the systematic improvement of biomimetic peptide-mediated strategies for the controlled growth of inorganic nanomaterials in environmentally benign conditions lies in the lack of clear conceptual connections between the sequence of the peptide and its surface binding affinity, with binding being facilitated by non-covalent interactions. Peptide conformation, both in the adsorbed and non-adsorbed state, is the key relationship that connects peptide-materials binding with peptide sequence. Here, we combine experimental peptide–titania binding characterization with state-of-the-art conformational sampling *via* molecular simulations to elucidate these structure/binding relationships for two very different titania-binding peptide sequences. The two sequences (Ti-1: QPYLFATDSLIK and Ti-2: GHTHYHAVRTQT) differ in their overall hydropathy, yet *via* quartz-crystal microbalance measurements and predictions from molecular simulations, we show these sequences both support very similar, strong titania-binding affinities. Our molecular simulations reveal that the two sequences exhibit profoundly different modes of surface binding, with Ti-1 acting as an entropically-driven binder while Ti-2 behaves as an enthalpically-driven binder. The integrated approach presented here provides a rational basis for peptide sequence engineering to achieve the *in-situ* growth and organization of titania nanostructures in aqueous media and for the design of sequences suitable for a range of technological applications that involve the interface between titania and biomolecules.

Keywords: peptides, titania, adsorption, molecular dynamics simulations, bio-interfaces

Introduction

The recognition of nanostructured inorganic materials by biomolecules such as peptides is an intriguing phenomenon found throughout nature, which, if exploited systematically, promises transformative applications in materials science.[1-4] Use of bioinspired approaches to realize the nucleation, growth and functionalization of materials in aqueous media, principally by the addition of peptides[5-6] shows exciting promise, and has become the subject of intense scrutiny for a range of materials[7], such as noble metals,[8-9] graphene[10-11] and silica,[12] in addition to titania (TiO_2).

TiO_2 (titania) is an attractive material for use in medical and environmental applications[13] due to its optical, adsorbent and catalytic properties[14] and also its moderately benign interface with biological matter, leading to its widespread use in biomedical implant materials.[15-16] Peptide-based approaches to the generation of nanostructured titania are therefore of current interest. However, a significant obstacle to developing versatile and reliable peptide-based strategies for the generation and organization/activation of nanostructured inorganic materials is our limited understanding of how to exploit the relationship between peptide sequence and corresponding materials-binding affinity.[5, 17] To this end, a deeper understanding of the physical provenance of peptide-materials recognition is much needed to advance protocols for the peptide-based generation and organization of nanostructured inorganic materials.

Several experimental and computational studies have focused on the fundamentals of recognition between titania and amino acids,[18-25] for which much (but not all – see the work of *e.g.* McQuillan and co-workers[18]) of the experimental work has been done *in vacuo*, which is most probably not directly relevant to aqueous conditions. Overall, the broad view from these experimental and simulation studies indicate that charged (R, K, D, E) and to a lesser extent polar (S, T, N, Q, Y) amino acids show the greatest degree of titania adsorption, while hydrophobic residues (V, L, I, F) exhibit negligible to zero binding affinity; simulations[19, 23] suggest that these residues actually have a *repulsive* interaction with aqueous titania. In particular, the fact that negatively-charged amino acids, such as aspartate and glutamate, can adsorb appreciably to a negatively-charged aqueous titania interface is counter-intuitive at first glance, but has been confirmed by previous experimental studies (see for example McQuillan and co-workers[18]),

and was supported by subsequent molecular dynamics simulations that quantified the free energy of adsorption and the associated binding structures at the interface.[19] These simulation data suggested that this phenomenon could be ascribed to the nanoscale patterning of partial positive charge and negative charge, inherent to the presentation of both Ti and H, and O atoms at the surface. The resulting charge density arises from the number of negatively-charged patches outweighing the number of positively-charged sites, while the positively-charged regions are the likely adsorption sites for the negatively-charged adsorbates. While these studies have yielded valuable insights, it is now clear that the interplay between sequence, structure and interfacial adsorption is not an additive sum resulting from the presence of "strong binding" residues in a peptide sequence.[5, 17] Therefore, the investigation of entire peptide chains in contact with inorganic surfaces is a critical component in advancing our understanding.[26] The tri-peptide motif RGD and its interaction with titania surfaces has been of particular interest,[27-33] while others have sought to isolate and identify TiO_2-binding peptides using biocombinatorial techniques to gain a deeper understanding of which peptide characteristics can confer strong titania-binding affinity.[32, 34-37]

A crucial next step in advancing our understanding is the careful characterization of the adsorption of materials-binding peptides at aqueous titania interfaces.[36-37, 39-43] Of particular note is the work of Yazici *et al.*[36] who used quartz crystal microbalance (QCM) measurements to determine the binding free energy of three sequences; two "strong-binders", RPRGNRGRERGL and SRPNGYGGSESS, with ΔG_{ads}= -34.5 and -38.5 kJ mol^{-1} respectively and one "weak-binder", VGRVTSPRPQGR, with ΔG_{ads}= -27.6 kJ mol^{-1}, identified from cell-surface display screening experiments. We note that these measurements were done in phosphate buffered saline solution, and their binding target was a Ti film generated using chemical vapour deposition, chemically similar to implant-grade Ti, while the target for their cell-surface display experiments was implant grade titanium with a naturally oxidized layer. Yazici *et al.* found that overall sequence charge was *not* a determining factor, with both positively-charged and charge-neutral sequences appearing in their set of "strong-binders". The presence of basic and polar residues in their "strong-binder" sequences, along with the presence of hydrophobic residues in their "weak-binder" sequence, is consistent with predicted amino acid binding free energies previously reported by us.[19, 23] In particular, our previous

amino acid binding free energy predictions indicate that hydrophobic residues have an entirely repulsive interaction with the aqueous titania interface, and therefore seek a location as far as possible from the interface.

However, Yazici *et al.* did not report any experimental structural data for these sequences beyond circular dichroism (CD) spectroscopy, which indicated that each sequence was intrinsically disordered, with a strong degree of random coil character. The results of their molecular dynamics (MD) simulations related only to the free (unadsorbed) peptide and were generated under implicit solvation conditions using insufficient conformational sampling, followed by energy-minimization of lowest-energy candidates in explicit solvent (liquid water). As we demonstrate herein, this simulation procedure is inadequate and cannot reliably capture the conformational ensemble of these molecules; these findings should therefore be interpreted with caution. To this end, the more general links between sequence, structure and binding remain to be elucidated for Ti-binding peptides.

However encouraging, these previous studies have not yet provided the level of in-depth comprehension at the molecular-level required to accomplish the rational manipulation of peptide-titania recognition. This shortcoming can be attributed to the lack of complementary studies that are able to connect the peptide sequence to its binding affinity *via* knowledge of the structural ensemble of the adsorbed peptide. Such detailed structural data, while enormously valuable, are challenging to either obtain or interpret for peptides adsorbed at inorganic materials interfaces.[44] On one hand the results for CD spectroscopy can be readily obtained but are ambiguous to interpret for such short peptides;[37] alternatively, while nuclear magnetic resonance (NMR) spectroscopy data can be more readily interpreted, these can be challenging to generate.[45] Advanced molecular simulation approaches are capable of providing these molecular-level details, as was recently shown for the prediction and elucidation of the facet-selective binding preferences of peptides at aqueous Au interfaces.[46] Therefore, molecular simulation, when carefully performed, and done in close partnership with experimental approaches, can bring valuable insights into the structure-binding relationships inherent to these versatile and widely-used materials.[17, 23, 47-49]

Here, we have examined the binding behavior of two TiO_2 binders, Ti-1 and Ti-2, previously used in the biomineralization of crystalline, sub-10 nm sized TiO_2 nanoparticles from water (pH 7.4) or Tris buffer particles[37] (see Table 1 for peptide sequences). The peptides were originally identified by panning against 100 nm titanium nanoparticles.[37] Our two peptide sequences differ substantially in terms of the overall balance between hydrophobic residues and charged residues. In this study we quantified the thermodynamic and structural aspects of adsorption for these two titania-binding peptides at a negatively-charged aqueous titania interface, using a close partnership of experimental and molecular simulations employing advanced conformational sampling approaches. These data revealed that although Ti-1 and Ti-2 exhibit very similar titania-binding strengths, these two sequences achieve this *via* profoundly different modes of surface adsorption.

Materials and Methods

Peptide Synthesis. Sequence Ti-2 was synthesized in house by microwave-assisted solid-state synthesis using an automated pep-tide synthesizer (CEM), and characterized by HPLC (pu-rity >90%) and mass spectrometry. Sequence Ti-1 was obtained from Pepceuticals (purity >85%).

QCM Surface Binding Analysis. Quantitative binding affinity measurements were made using a Q-sense E4 QCM-D with flow modules. QCM sensors coated with 100 nm titanium (Q-sense, QSX-310) were cleaned by UZ/ozone treatment (Novascan PSD Pro Series Digital UV/Ozonesystem) for 10 min, followed by immersion in a 2% SDS solution for 30 min, thorough rinsing with de-ionized water, N_2 drying, and another UZ/ozone treatment for 10 min. After cleaning, sensors were mounted in QCM flow modules, and Ti-1 and Ti-2 peptides of varying concentration were flowed across the sensors at a rate of 0.17 mL/min at 23°C. Peptide solutions were made up using water (pH adjusted to 7.4 with NaOH 0.01 M) and then NaCl added to give the 0.15 M NaCl solution. The latter solution was to mimic conditions used in the initial phage display experiments that identified the peptides[37] and also of more relevance to the behavior of titanium based materials used as implants in the human body. The third overtone frequency was

measured and used to calculate the adsorbed and desorbed mass of peptide and other ions/ water using the Sauerbrey equation.[58-59] Using QCM-D, the Gibbs free energy is experimentally accessible through measurement of the initial rates of adsorption. The adsorption curve of each peptide at varying concentrations was fitted using a Langmuir isotherm, allowing values for k_{obs} to be determined.[5] By utilising QCM-D data, the layer thickness of the peptide overlayer can be approximated[60] provided the effective density of the adhering layer is known. This density value was estimated by implementing the method reported by Fischer *et al*.[61] Full details of these calculations are provided in "Overlayer Thickness Estimates from QCM-D data" in the Supporting Information.

Molecular Dynamics Simulations Details. All of our REST simulations[53-54] described herein used the CHARMM22* force-field[62-63] for the peptides and the modified TIPS3P model[64] was used for liquid water. The protonation state of the residues was set to those consistent with a pH of 7. In the case of the His residues in Ti-2, which can be found in both the protonated and unprotonated states at pH 7, we set up H2 and H6 in the unprotonated state, while H4 was modeled in the protonated state. Further details and discussion on this choice are provided in the "Additional Computational Methodology" section of the Supporting Information.

REST-only Simulations. For the "surface-adsorbed" REST-only simulations, one chain of either Ti-1 or Ti-2 was modeled in the presence of the negatively-charged, hydroxylated aqueous rutile TiO_2 (110) interface, carried out using GROMACS 4.5.5[66] in the *NVT* ensemble. The Predota force-field[67] was used to model the titania surface. Ions (Na^+ and Cl^-) were added to the solvent such that the concentration of NaCl in bulk solution was 0.15 M. We also performed REST-only simulations of each of these peptides in aqueous solution in the absence of the titania slab. For these "in solution" REST-only simulations, we modeled one chain of either the Ti-1 or Ti-2 peptide in a cubic simulation cell along with liquid water and Na^+ and Cl^- ions to ensure a Na^+ concentration of 0.15 M. Further details of the REST simulations, including details of the surface model, and full details of the trajectory analysis (residue-surface contact

analysis, clustering analysis, *etc*) are provided in the Supporting Information, 'Additional Computational Methodology'.

REST+MetaD Simulations. Two REST+MetaD simulations were performed, one for each peptide adsorbed at the negatively-charged aqueous rutile TiO_2 (110) interface. The simulations were carried out using GROMACS 4.5.5, coupled with an in-house customized version[46] of the PLUMED 1.3 plugin.[68] Each REST+MetaD simulation was run for 120ns, which is approximately equivalent to μs-long standard MD simulations.[46] Here, a single collective variable (CV) was used, namely the vertical distance normal to the titania surface plane between the peptide center of mass and the titania surface, defined by the top Ti atoms of the slab. Gaussian hills of height 0.2 kJ mol^{-1} and width 0.1 Å were added along the CV direction every 0.5 ps. Other details of the REST+MetaD simulations were identical to those used in the REST-only simulations at the titania interface. Additional methodology concerning the extraction of the adsorption free energy are provided in the Section "Additional Computational Methodology" in the Supporting Information.

Information on alternative simulation strategies based on REMD in implicit solvent and molecular dynamics in explicit solvent (0.15 M sodium chloride) are provided in the Supporting information.

Results and Discussion

The sequences Ti-1 and Ti-2 share similarities in their overall charge characteristics compared with the "strong-binder" sequences reported by Yazici *et al.*,[36] Ti-1 is charge-neutral overall, featuring both positively-charged and negatively-charged residues, while Ti-2 carries an overall positive charge, including one Arg and several His residues. The overall hydropathy of the two sequences is also markedly different, with Ti-2 predicted to be significantly more hydrophilic, while Ti-1 shows slight hydrophobic character. As we shall show below, these two peptide sequences are indicated to be intrinsically disordered with substantial random coil characteristic of their respective conformational ensembles.

QCM Binding Analysis. A quantitative measure of binding affinity and dissipation energy associated with the binding of peptides of Ti-1 and Ti-2 to naturally oxidized titanium was investigated using QCM-D measurements, with a Ti sensor as the binding target. As described by Tang *et. al,*[5] the binding affinity of

a particular sequence is characterized by the difference in Gibbs free energy between the bound and unbound states, $\Delta G = \Delta H - T\Delta S$, which is related to the equilibrium constant for binding, $K_{eq} = \exp[\Delta G/(RT)]$, where T denotes temperature. In previous studies, the high affinity of both peptides for TiO_2 surfaces was suggested to be responsible for the formation of nanometer-sized crystalline nanoparticles of titania *via* a capping mechanism.[37] We have shown previously that phosphate ions interfere with such a mechanism and lead to the generation of larger phosphate-containing particles. A summary of our QCM-D adsorption data, both for peptide in water at pH 7.4 and 0.15 M NaCl solution at the same pH (see Methods) is presented in Figures 1 and 2 and Table 2.

Exemplar QCM-D data for Ti-2 adsorption to the Ti-sensor surface in 0.15 M NaCl solution (Figure 1b) show a negligible dissipation energy, suggestive of a single, rigid absorbed peptide layer present on the Ti sensor surface. The adsorption free energy (ΔG) of Ti-2 in 0.15 M NaCl is calculated to be -39.19 kJ mol^{-1}. This binding free energy is comparable to that obtained for the gold binding peptide AuBP1[5] (WAGAKRLVLRRE) adsorbed at the aqueous Au interface (-37.6±0.9 kJ mol^{-1}). The binding energy of Ti-2 in water at the same pH is slightly lower, but still substantial at -32.90 kJ mol^{-1}.

The adsorption of Ti-1 to the titania coated titanium sensor in water at pH 7.4 gave a similar binding free energy, statistically equivalent to that of Ti-2 under the same experimental conditions (Table 2). In contrast, the initial adsorption behavior for all concentrations of Ti-1 in 0.15 M NaCl solution followed a linear trend (Figure 1a) that was not amenable to Langmuir model analysis (suitable for a bound monolayer), nor to a Freundlich model (bound multilayers) analysis. These results suggest that the initial adsorption mechanism of Ti-1 differs from Ti-2 in the presence of 0.15M NaCl solution. This is not the first time that such a pattern of binding behavior has been observed[50] for titania binding peptides: in addition, in this prior study, the authors were unable to account for the trend in binding behavior.[50]

Figure 2, Table 3, and Table S1 in the Supporting Information provide further insight into the difference in adsorption and desorption behavior of the two peptides under the two solution conditions used for the binding experiments. Differences in the amount of surface-bound mass (even allowing for the fact that QCM measures the mass of liquid and ions adsorbed as well as the analyte (the peptide in this study)) as

well as the rates of adsorption and desorption (Table S1) were measured. We also considered the possible thickness of the peptide overlayer on the sensor surface, and the consequences for this in terms of the possible packing of peptides on the surface and their concomitant inter-peptide interactions. The layer thickness for Ti-1 and Ti-2 in NaCl was estimated[60-61] at ≈ 7 Å and ≈ 13 Å respectively. We combined these estimates with two extremes of an idealized peptide surface arrangement in the adsorbed state; the horizontally-oriented state, and the vertically-oriented state, see Figure S1a in the Supporting Information. This allowed us to deduce that the peptides are likely to be lying in a horizontal arrangement on the sensor surface. Layer thickness estimations can be compared with the REST-only simulations (*e.g* see Figure 3), in which the distance between the peptide centre-of-mass and the titania surface is within the range of ~8-12 Å, indicating a reasonable agreement between the simulation data and experimental data. The data in Table S2 and Figure S1 also suggest that the mass adsorbed for Ti-1 and Ti-2 is expected to result in an extremely sparse monolayer coverage. An assessment of the extreme idealized horizontal and vertical modes indicated that Ti-1 could adsorb in approximate isolation within an average area ≈23× greater than its ideal surface area in the horizontal case, or ≈120× greater than its ideal surface area in the vertical case. Layer thickness estimations can be compared with the REST-only simulations shown in Figure 3. The film thickness for Ti-1 and Ti-2 in water was similarly estimated at ≈ 42 Å and ≈ 30 Å respectively, which is significantly greater than that estimated for NaCl solution. However, the increase in energy dissipation in water indicates that the peptide layer may be more viscoelastic in nature, and concomitantly the adsorbed mass/thickness may be underestimated by the Sauerbrey relation.

For experiments performed in the presence of 0.15 M sodium chloride, for both sequences, the peptide was observed to remain on the sensor after 0.15 M NaCl was reintroduced into the system, Figure 2a. Furthermore, Ti-2 remained on the sensor surface after water (pH 7.4) was reintroduced, Figure 2b. For both peptides, there was a significantly smaller amount of material adsorbed to the surface from the 0.15 M NaCl solution compared to adsorption from water; with similar behavior being reported previously on the binding of these peptides to a Ti sensor in the presence of a phosphate buffer.[37] The rate of peptide

adsorption onto the Ti-sensor surface was lower from 0.15 M NaCl solution compared to peptide adsorption from water at pH 7.4 (Table S1, Supporting Information). Reintroduction of a salt-only wash to the Ti-1 system was only able to remove *ca.* 25% of the material bound; this was in distinct contrast to the behavior observed for Ti-1 in water, where after addition of a pH 7.4 water wash, all of the bound Ti-1 desorbed.

This difference in behavior for Ti-1 in the two solutions (0.15 M salt and water at pH 7.4) may be attributed to a preference for the peptides to solvate in water compared to the salt solution where it is more likely the peptides are salting out of the solution. The negligible dissipation energy observed for 0.15 M NaCl, suggests a single, rigid absorbed peptide layer is formed whilst the increase in energy dissipation in the water indicates the peptide layer to be soft/viscoelastic. The nature of these contrasting types of interfacial layer may also contribute to the explanation of the response of the system observed upon the reintroduction of washing buffer. The larger, softer layer formed in H_2O would be prone to disruptions during washing while a smaller rigid film may not be as exposed during washing. In H_2O buffer conditions, for both Ti-1 and Ti-2, dissipation energy data, Figure 2b, indicated that a secondary layer was formed during adsorption, and desorption of the peptide in the case of Ti-1 may be driven, at least in part by the presence of a large number of hydrophobic amino acid residues, which is in agreement to what was observed by McQuillan *et al.*[18] and as was found for a purely hydrophobic peptide AFILPTG from a silica surface.[51]

In summary, peptides Ti-1 and Ti-2 show different adsorption/desorption behavior in water (pH 7.4) and salt (0.15M) which can in part be ascribed to differences in their chemical properties, including the numbers of charged and hydrophobic residues. Precisely how they bind to the titania surface, including information on the specific amino acids involved and their likely conformation cannot be obtained from the experimental studies alone.

Advanced Sampling Molecular Dynamics (MD) Simulations. We next carried out detailed molecular simulations to elucidate the links between sequence and binding behavior. Herein, we show that Ti-1 and

Ti-2 are intrinsically disordered. Intrinsically disordered peptides are not represented by any single peptide "structure"; they support a range of different conformations. From a molecular simulation perspective, prediction of a single structure for an IDP is essentially a meaningless result. As indicated by our previous work,[5-6, 52] the Boltzmann-weighted conformational ensemble of intrinsically-disordered peptides is anticipated to be complex. This complexity requires the use of advanced conformational sampling, as detailed below.

We start with our simulations of the peptides adsorbed at the aqueous, negatively-charged titania interface to quantify and characterize peptide-surface adsorption at the molecular level. To accomplish this, we performed two sets of advanced sampling simulations, based on Replica Exchange with Solute Tempering (REST) MD simulations.[53-54] First, we implemented state-of-the-art REST+Metadynamics (REST+MetaD) simulations to obtain estimates of the free energy of peptide-titania adsorption; a quantity that is extremely challenging to capture using molecular simulation.[46] In addition, we performed REST-only simulations to determine the conformational ensemble of each peptide in the adsorbed state, and to reveal the surface-contact preferences of each residue in each peptide. While in principle these data could be extracted from the REST+MetaD simulations, in practice, this is an extremely challenging task, and the outcomes of this analysis are not necessarily definitive; resolution of this issue remains for in future developments.[46]

For both Ti-1 and Ti-2, we obtained the change in free energy as a function of the peptide–surface distance, from which the adsorption free energy was extracted and compared. This was accomplished *via* construction of symmetrized free energy profiles[46] (see 'Additional Computational Methodology' in the Supporting Information); see Figure 4 for an exemplar symmetrized free energy profile. The predicted free energy of adsorption for the two peptides was found to be **-12.7±0.4** kJ mol^{-1} and **-16.4±3.7** kJ mol^{-1} for Ti-1 and Ti-2 respectively. Our predicted adsorption free energies are therefore very similar in magnitude for the two sequences, with overlapping error bars signifying these free energies are very close in value. Statistical analysis *via* a *t*-test was not conclusive in providing definitive evidence that the values

were significantly different. While the absolute value of each experimental adsorption free energy does not agree with the corresponding predicted value, our simulations support the same *trend* in binding free energies (Table 2), with both peptides adsorbing with similar affinity. We provide evidence of the approach to equilibration for our REST+MetaD simulations in the form of histograms of the sampled CV as a function of timestep, as well as the evolution of the free energy profiles, and evolution of adsorption well-depth (Figures S2-S4 in the Supporting Information). Further discussion regarding the free energy analysis, in particular with respect to the location of the dividing surface between unadsorbed and adsorbed states, and the dimension of the simulation cell perpendicular to the slab surface, is provided in the Supporting Information, in the "Additional Computational Methodology" section.

The REST+MetaD approach recently demonstrated the reproduction (within error) of the absolute value of the experimentally-measured binding free energy of the AuBP1 sequence adsorbed at the aqueous polycrystalline Au interface.[46] For our simulations reported here, we propose several factors that may account for the difference in the absolute values observed in experiment and those predicted from our simulations; our structural model of the aqueous titania interface, the force-field used in our simulations, and the neglect of multiple-chain effects in the adsorbed state. Regarding the structural model, we have approximated the unknown structure of the naturally-oxidized titanium surface used in the experiments with a partially-hydroxylated, negatively-charged rutile TiO_2 (110) surface (see Figure S5 and Section 'Additional Computational Methodology' in the Supporting Information). This particular structural model was reported to support very good agreement between predicted[19] and experimentally-observed[18, 34, 55-56] amino acid binding free energies, particularly in the cases where the experimental surface was predominantly the crystalline rutile (110) surface, although the predicted data were also consistent with experimental data reported for amorphous titania surfaces.[56] Therefore, while our surface model may, to first approximation, provide a reasonable description of the experimental system, some differences between the QCM data and our predictions are expected, which may be due both to the particular phase of titania modeled here, and to the underlying geometrical features of the (110) surface.

Regarding the force-field (FF), we recognize that one unavoidable limitation of the present work is the use of a non-reactive FF. While our particular combination of force-fields shows excellent agreement with a range of different experimental observations (see Sultan *et al.*[19] and discussion therein), recent simulation studies have suggested that proton transfer can be an important effect on the interaction of biomolecules with titania interface – see for example the recent work of Monti *et al.*[69] At present, the substantial overhead in computational cost associated with use of such reactive FFs would make our REST+MetaD simulations impracticable. Furthermore, as opposed to a FF such as CHARMM, such reactive FFs suffer from a lack of development and validation for the simulation peptides, and therefore the incorporation of reactivity would almost certainly compromise the reliability of the description of the potential energy landscape of the peptide.

Regarding the neglect of multiple-chain effects in the adsorbed state, there are numerous aspects to consider, which are discussed below. Although estimates from our QCM data do not indicate a closely-packed peptide overlayer in the surface-adsorbed state (*vide supra*), we nonetheless recognize the possible influence of the presence of several peptide chains in the surface-adsorbed state (i.e. a multi-chain overlayer) on our simulation predictions, which model the single-chain surface-adsorbed peptide. The possible interplay between the inter-peptide interactions and the peptide-surface interactions have not been considered here; currently consideration of these factors present substantial challenges from both experimental and molecular simulation perspectives, both in terms of determining binding free energies and binding structures.

For the former, calculation of peptide-binding free energies for a peptide overlayer is a challenging task to realize from a computational perspective. There are no known reports of the use of sensible conformational sampling strategies (*i.e.* metadynamics based approach or equivalent) to determine how the free energy of adsorption changes for a peptide adsorbed in a multi-chain (monolayer or sub-monolayer coverage) configuration. From an experimental perspective, limited data are available. We point to the work of Latour and co-workers, who were able to correct for intra-peptide interactions in their

surface plasmon resonance-based evaluation of peptide/self-assembled monolayer binding free energies.[70] This study demonstrated two key points relevant to this discussion: 1) the inter-peptide-interaction corrections on their binding data were small, and in the "strong binding" regime were roughly constant at ~6 kJ mol^{-1}, and 2) the shift in corrected free energies in the "strong binding" regime was only in one direction, and meant the uncorrected binding affinities were stronger than they should have been, not weaker. Therefore, on the basis of Latour and co-workers' findings, we would conclude that peptide-peptide interactions do have the capability to modulate the peptide-surface adsorption strength, but the available evidence indicates this is a small effect.

For the latter, we emphasize that currently it is very challenging to experimentally establish coverage and structural data of peptide overlayers adsorbed on materials surfaces under aqueous conditions – the experimental (mostly atomic force microscopy, AFM) data in the literature pertaining to this phenomenon are typically taken from dried samples (see *e.g.* So et al.[71]). Unfortunately such AFM data are not representative of the bound peptide structure(s) in water. Unambiguous experimental evidence of the structure of the adsorbed peptide overlayer in solution would require AFM imaging in solution with near atomic-scale resolution; to date this remains an unresolved grand challenge in the field. In summary, a detailed evaluation (either *via* experimental observation or computational prediction) of the spatial distribution of peptides in a multi-chain overlayer-adsorbed state is a much larger and complex question that is outside the scope of this current work, which will demand a concerted and systematic effort from both experimental and computational approaches for many years to come.

To elucidate the structural origins of this similarity in binding free energies, we analyzed trajectories from our REST-only simulations of the Ti-1 and Ti-2 peptides adsorbed at the aqueous rutile TiO_2 (110) interface. As explained previously, both Ti-1 and Ti-2 are expected to support a complex ensemble of thermally-accessible conformations, both in the presence and absence of the titania interface. We classified the peptide conformations in the ensemble according to similarity in backbone structure (using a clustering approach, see 'Additional Computational Methodology' in the Supporting Information). This

analysis generates the set of most likely structures (referred to herein as 'clusters') and their respective relative populations in the ensemble. Intuitively, a strong peptide-surface binding affinity can arise from binding enthalpy considerations, such as the probable number, distribution, and type of residue-surface contacts.[5] Additionally, our previous work suggests that strong binding affinity can also arise from the system possessing many different adsorbed conformations, of which the degree of disorder in the adsorbed state is an indicative metric.[5] Our clustering analysis provides an estimate of this degree of disorder in the surface-adsorbed state. In this sense, the favourable binding energy of Ti-1 is in part facilitated by the large number of thermally-available, structurally-distinct adsorbed peptide conformations. Structures representing the most likely adsorbed conformations (the cluster with the highest population) are shown in Figure 3 for the two adsorbed peptides (see also Figure S6 in the Supporting Information). As an indication of the convergence of our clustering analysis, in Figure S11 in the Supporting Information we provide the number of clusters as a function of REST MD steps. These data show that by ~12 x 10^6 REST simulation steps the number of unique thermally-accessible conformations has started to plateau.

The population of the top (most populated) cluster (shown in Figure 3) is ~12% and ~23% of the ensemble for Ti-1 and Ti-2 respectively, with the full list of population distributions provided in Table S3 of the Supporting Information; these data are clearly indicative of intrinsic peptide disorder[5]. The total number of clusters in each case (182 and 113 for Ti-1 and Ti-2 respectively), indicative of the number of thermally-accessible, distinct surface adsorbed conformations at room temperature, suggests that Ti-1 features a greater amount of structural disorder. As an independent check of the structural disorder of these surface-adsorbed peptides, we have also used the Schlitter-entropy formula[72], applied to the positions of the peptide backbone atoms, to estimate the conformational entropic contribution to the binding. We obtained values of 807.6 and 750.2 J K^{-1} mol^{-1} for Ti-1 and Ti-2, respectively. Further data such as Ramachandran analyses (Figure S7 of the Supporting Information) provide further evidence of the random coil nature of each adsorbed peptide.

In Figure 3, we also show the variation in the averaged interfacial water density, revealing how the peptide side-chains may interact both directly with the titania surface and with the first structured layers of interfacial water (referred to herein as 'direct' and 'solvent-mediated' adsorption respectively). This tendency of aqueous titania to support two binding modes (one mediated *via* interfacial solvent structuring) has been reported previously.[49,57] To analyze these adsorption modes in greater depth, we calculated histograms of residue-surface distance for both Ti-1 and Ti-2, provided in Figure S8 in the Supporting Information. These data clearly indicate the preference of some residues to interact *via* the first interfacial water layer.

To quantify the degree and distribution of residue-surface contact, we calculated the fraction of the REST-only trajectory that each residue spent in 'direct' contact with the surface, as summarized in Figure 5. These data, along with a detailed analysis of the 'solvent-mediated' contact (see Table S4 in the Supporting Information for numerical values) reveal a profound difference in binding modes between the two peptide sequences, despite the predicted similarity in adsorption free energies. In particular, Ti-1 featured very limited direct surface contact, with the polar residues in the chain center and the acidic D8 residue not participating in surface binding to a significant extent. This lack of predicted surface contact for D8 is somewhat surprising considering that fact that the Asp amino acid is thought to bind to titania.[18-19] This result highlights the fact that the peptide sequence and concomitant peptide conformation can modulate how the interaction of a *residue* with an interface, compared with that of the corresponding *amino acid*. In Ti-1, the epitope of direct binding instead comprises the chain ends, assisted by K12, which due to the relatively long side-chain, can still make direct surface contact despite the peptide backbone being distant from the interface. On the basis of this evidence, together with the estimates of the degree of conformational disorder (from both the clustering analysis and our calculations of the Schlitter entropy), we classify Ti-1 as an entropically-driven binder.[5] In this sense, the favorable binding free energy of Ti-1 is in part facilitated by the large number of thermally-available, structurally-distinct adsorbed peptide configurations. Inspection of the peptide sequence provides clues to the origin of this

binding behavior, particularly the fact that D8, which in principle should act as a strongly-binding residue, is effectively reduced to the role of a spectator in Ti-1. We attribute this to the fact that the T7-D8-S9 motif is flanked by substantive hydrophobic content; these flanking hydrophobic residues give rise to repulsive interactions[19] that prevent the close approach of this motif to the surface.

In contrast, our residue-surface contact analysis for Ti-2 (Figure 5, and Figure S8 and Table S4 in the Supporting Information) shows extensive direct interaction with the surface, distributed almost evenly across the sequence. As expected[19], R9 and the chain ends are indicated as the most likely contact points. In addition, our clustering analysis of the surface-adsorbed conformations of Ti-2 (Table S3 in the Supporting Information) suggests relatively fewer thermally-accessible adsorbed conformations compared with Ti-1. Taken together, these data for Ti-2 suggest classification of Ti-2 as an enthalpically-driven binder[5], with the favorable binding free energy attributed chiefly to the strong enthalpic residue-surface contact.

We also characterized the conformational ensemble of the non-adsorbed peptides (in the absence of the titania surface) *via* REST-only[53-54] simulations in explicit solvent for both Ti-1 and Ti-2. The most populated clusters, shown in Figure 6 and Figure S9 in the Supporting Information, are lacking in clear secondary structure motifs, while the cluster populations and the total number of clusters (provided in Table S3 of the Supporting Information) again indicate intrinsic disorder.[5] As identified for the surface-adsorbed systems, we found that in the unadsorbed state Ti-1 featured a greater amount of disorder than Ti-2, where the total number of clusters was found to be 270 and 200 for Ti-1 and Ti-2 respectively. Calculations using the Schlitter-entropy formula for the peptide backbone atoms corroborated our clustering analysis, with values of 857.8 and 846.8 J K^{-1} mol^{-1}, for Ti-1 and Ti-2 respectively. The total number of thermally-accessible peptide structures for each sequence in the absence of the surface is greater than that found for the corresponding surface-adsorbed environment; 270/182 respectively for Ti-1, and 200/113 respectively for Ti-2.

Both peptide sequences were previously reported[37] to show significant variation in CD spectral response when in the presence of titanium bisammonium lactatodihydroxide (TiBALDH), a TiO_2 precursor compared to their behavior in the absence of the titania precursor (re-presented here in Figure 7 for convenience). Both Ti-1 and Ti-2 were found to be random coil in solution and upon precursor/surface interaction; however, the spectral changes were noted to be more marked for Ti-1. These experimental data are consistent with the prediction of higher susceptibility of Ti-1 to conformational change upon interaction with a surface.

Finally, we also directly compared each distinct conformation (cluster) between the in-solution and surface-adsorbed environments for each peptide sequence (see Tables S5 and S6 in the Supporting Information). These data identified structural matches between each in-solution cluster with clusters found in the surface-adsorbed state, for a given peptide sequence. Only two notable matches (involving clusters with non-negligible populations) were found for Ti-1 (cluster numbers 3 and 4, and clusters 5 and 8, for in-solution and surface-adsorbed states respectively). In contrast, a similar analysis for Ti-2 revealed an extensive degree of similarity between the top-ten most populated clusters of both the in-solution and surface-adsorbed states. These data suggest that the Ti-1 sequence is inherently more susceptible to change in conformation upon exposure to the surface, while Ti-2, to a relatively greater degree, retained the structural characteristics of the solution-based conformational ensemble in the surface-adsorbed state.

Some comments on our analysis of the REST-only simulations are warranted. Our clustering analysis allows an estimate of the conformational contribution to the binding entropy. While in principle there are approaches to directly calculate both the binding enthalpy change and the binding entropy change, in practice, these are currently impracticable for obtaining a decisive resolution. Specifically, while the enthalpy of binding can in principle be obtained from the difference in the potential energy of the adsorbed and unadsorbed states, in practice this strategy has a number of challenges that render it impractical at present, as outlined in a recent study.[73] While it may be possible in principle to obtain the binding enthalpy and binding entropy changes from the van't Hoff equation, this strategy is impractical, because it requires

the calculation of the free energy of adsorption at several temperatures. Even if the enormous computational expense in using REST+metaD simulation was not a factor, anecdotal experience (for smaller molecular adsorbates) indicates that the resulting errors, especially for the entropy term, are too large for any meaningful conclusions to be drawn.

To highlight the importance of comprehensive conformational sampling in the presence of liquid water when modeling these peptides, we also carried out Replica Exchange MD simulations of each peptide chain in implicit solvent. The most likely predicted structures from these implicit-solvent REMD simulations were subsequently immersed in 0.15 M NaCl solution and subjected to standard MD simulation. This approach resulted in predictions of over-structuring, chiefly attributed to the formation of helices in the implicit solvent simulations, which persisted once these structures were transferred into a liquid water environment (see 'Implicit Solvent Simulations' in the Supporting Information for methodology and results). These findings highlight that data generated using such approaches, for instance those published previously[36], should be interpreted with caution. Implicit-solvent models, even when followed up with explicit solvation simulations, should not be used to characterize the conformational ensemble of materials-binding peptides.

Our combined experimental and simulation analyses suggest that the two titania-binding sequences, Ti-1 and Ti-2, which we have shown by both approaches to have very similar surface binding affinities, accomplished surface binding *via* dramatically different adsorption modes. The binding behaviors of Ti-1 and Ti-2 are consistent with the two categories of strong materials-binding behavior proposed in previous work for Au-binding peptides[5], namely the 'enthalpic binder' and the 'entropic binder'. Ti-2 did not support a relatively large number of adsorbed states, but in each of these states featured a set of strong, non-covalent residue contact points with the surface that were positioned throughout the sequence. In contrast, Ti-1 supported a much greater number of adsorbed states, with each possessing a relatively lesser degree of peptide-residue contact.

Conclusions

In summary, we have combined an experimental quantification of the peptide-surface binding strength for two very different peptide sequences, Ti-1 and Ti-2, adsorbed at the aqueous titania interface, with advanced molecular simulations, to elucidate the structure/binding relationships of these sequences. Despite containing a substantial amount of hydrophobic content, Ti-1 was found to bind approximately as strongly as Ti-2. This binding behavior was also indicated by our molecular simulations. On the basis of the predicted conformational ensembles and peptide-surface interactions, we propose two different binding modes for these peptides. Ti-1 is an entropically-driven binder, without the presence of strong, anchor residues, while Ti-2 is an enthalpically-driven binder, featuring a high number of almost periodically-spaced anchor residues along the chain length. Both modes of contact are capable of delivering strong surface binding. The different binding mechanisms result in distinctive adsorption/desorption behavior which was evidenced by QCM analysis. The combination of experimental and computational results presented herein provide a fundamental starting point for the rational manipulation of peptide sequence to engineer peptide sequences with desired titania-binding properties suitable for use in biomedical and other applications.

Acknowledgments: We gratefully acknowledge the Victorian Life Sciences Computation Initiative (VLSCI) for generous allocation of computational resources. TRW thanks **veski** for an Innovation Fellowship and acknowledges support from AFOSR grant FA9550-12-1-0226. AMS thanks Deakin University for a PhD IPRS scholarship. CCP is grateful to AFOSR for funding *via* FA9550-13-1-0040 and for access to the Odyssey cluster at Harvard University. Some of the computations in the supplementary section of this paper were run on the Odyssey cluster supported by the FAS Division of Science, Research Computing Group at Harvard University. MJB and TG acknowledge NIH U01 EB014976 and AFOSR FA9550-11-1-0199.

Supporting Information: Additional experimental and computational analyses discussed in the text. This material is available free of charge *via* the Internet at http://pubs.acs.org.

References

1. Care, A.; Bergquist, P. L.; Sunna, A., Solid-Binding Peptides: Smart Tools for Nanobiotechnology. *Trends Biotechnol* **2015**, *33*, 259-268.
2. Slocik, J. M.; Naik, R. R., Probing Peptide-Nanomaterial Interactions. *Chem Soc Rev* **2010**, *39*, 3454-3463.
3. Sarikaya, M.; Tamerler, C.; Jen, A. K. Y.; Schulten, K.; Baneyx, F., Molecular Biomimetics: Nanotechnology through Biology. *Nat Mater* **2003**, *2*, 577-585.
4. Dickerson, M. B.; Sandhage, K. H.; Naik, R. R., Protein- and Peptide-Directed Syntheses of Inorganic Materials. *Chem Rev* 2008, *108*, 4935-4978.
5. Tang, Z. H.; Palafox-Hernandez, J. P.; Law, W. C.; Hughes, Z. E.; Swihart, M. T.; Prasad, P. N.; Knecht, M. R.; Walsh, T. R., Biomolecular Recognition Principles for Bionanocombinatorics: An Integrated Approach to Elucidate Enthalpic and Entropic Factors. *ACS Nano* **2013**, *7*, 9632-9646.
6. Palafox-Hernandez, J. P.; Tang, Z. H.; Hughes, Z. E.; Li, Y.; Swihart, M. T.; Prasad, P. N.; Walsh, T. R.; Knecht, M. R., Comparative Study of Materials-Binding Peptide Interactions with Gold and Silver Surfaces and Nanostructures: A Thermodynamic Basis for Biological Selectivity of Inorganic Materials. *Chem Mater* **2014**, *26*, 4960-4969.
7. Evans, J. S.; Samudrala, R.; Walsh, T. R.; Oren, E. E.; Tamerler, C., Molecular Design of Inorganic-Binding Polypeptides. *MRS Bull* **2008**, *33*, 514-518.
8. Bedford, N. M.; Hughes, Z. E.; Tang, Z. H.; Li, Y.; Briggs, B. D.; Ren, Y.; Swihart, M. T.; Petkov, V.; Naik, R. R.; Knecht, M. R.; Walsh, T. R., Sequence-Dependent Structure/Function Relationships of Catalytic Peptide-Enabled Gold Nanoparticles Generated under Ambient Synthetic Conditions. *J Am Chem Soc* **2016**, *138*, 540-548.
9. Bedford, N. M.; Ramezani-Dakhel, H.; Slocik, J. M.; Briggs, B. D.; Ren, Y.; Frenkel, A. I.; Petkov, V.; Heinz, H.; Naik, R. R.; Knecht, M. R., Elucidation of Peptide-Directed Palladium Surface Structure for Biologically Tunable Nanocatalysts. *ACS Nano* **2015**, *9*, 5082-5092.
10. Kim, S. N.; Kuang, Z. F.; Slocik, J. M.; Jones, S. E.; Cui, Y.; Farmer, B. L.; McAlpine, M. C.; Naik, R. R., Preferential Binding of Peptides to Graphene Edges and Planes. *J Am Chem Soc* **2011**, *133*, 14480-14483.
11. Akdim, B.; Pachter, R.; Kim, S. S.; Naik, R. R.; Walsh, T. R.; Trohalaki, S.; Hong, G. Y.; Kuang, Z. F.; Farmer, B. L., Electronic Properties of a Graphene Device with Peptide Adsorption: Insight from Simulation. *ACS Appl Mater Inter* **2013**, *5*, 7470-7477.
12. Oren, E. E.; Tamerler, C.; Sahin, D.; Hnilova, M.; Seker, U. O. S.; Sarikaya, M.; Samudrala, R., A Novel Knowledge-Based Approach to Design Inorganic-Binding Peptides. *Bioinformatics* **2007**, *23*, 2816-2822.
13. Vallee, A.; Humblot, V.; Pradier, C. M., Peptide Interactions with Metal and Oxide Surfaces. *Accounts Chem Res* **2010**, *43*, 1297-1306.
14. Treccani, L.; Klein, T. Y.; Meder, F.; Pardun, K.; Rezwan, K., Functionalized Ceramics for Biomedical, Biotechnological and Environmental Applications. *Acta Biomater* **2013**, *9*, 7115-7150.
15. Liu, X. Y.; Chu, P. K.; Ding, C. X., Surface Nano-Functionalization of Biomaterials. *Mat Sci Eng R* **2010**, *70*, 275-302.
16. Khatayevich, D.; Gungormus, M.; Yazici, H.; So, C.; Cetinel, S.; Ma, H.; Jen, A.; Tamerler, C.; Sarikaya, M., Biofunctionalization of Materials for Implants Using Engineered Peptides. *Acta Biomater* **2010**, *6*, 4634-4641.
17. Skelton, A. A.; Liang, T. N.; Walsh, T. R., Interplay of Sequence, Conformation, and Binding at the Peptide-Titania Interface as Mediated by Water. *ACS Appl Mater Inter* **2009**, *1*, 1482-1491.
18. Roddick-Lanzilotta, A. D.; McQuillan, A. J., An in Situ Infrared Spectroscopic Study of Glutamic Acid and of Aspartic Acid Adsorbed on TiO_2: Implications for the Biocompatibility of Titanium. *J Colloid Interf Sci* **2000**, *227*, 48-54.

19. Sultan, A. M.; Hughes, Z. E.; Walsh, T. R., Binding Affinities of Amino Acid Analogues at the Charged Aqueous Titania Interface: Implications for Titania-Binding Peptides. *Langmuir* **2014**, *30*, 13321-13329.
20. Ataman, E.; Isvoranu, C.; Knudsen, J.; Schulte, K.; Andersen, J. N.; Schnadt, J., Adsorption of L-Cysteine on Rutile TiO_2(110). *Surf Sci* **2011**, *605*, 179-186.
21. Fleming, G. J.; Adib, K.; Rodriguez, J. A.; Barteau, M. A.; Idriss, H., Proline Adsorption on TiO_2(110) Single Crystal Surface: A Study by High Resolution Photoelectron Spectroscopy. *Surf Sci* **2007**, *601*, 5726-5731.
22. Wilson, J. N.; Dowler, R. M.; Idriss, H., Adsorption and Reaction of Glycine on the Rutile TiO_2(011) Single Crystal Surface. *Surf Sci* **2011**, *605*, 206-213.
23. Monti, S.; Walsh, T. R., Free Energy Calculations of the Adsorption of Amino Acid Analogues at the Aqueous Titania Interface. *J Phys Chem C* **2010**, *114*, 22197-22206.
24. Li, C.; Monti, S.; Carravetta, V., Journey toward the Surface: How Glycine Adsorbs on Titania in Water Solution. *J Phys Chem C* **2012**, *116*, 18318-18326.
25. Langel, W.; Menken, L., Simulation of the Interface between Titanium Oxide and Amino Acids in Solution by First Principles MD. *Surf Sci* **2003**, *538*, 1-9.
26. Costa, D.; Garrain, P. A.; Baaden, M., Understanding Small Biomolecule-Biomaterial Interactions: A Review of Fundamental Theoretical and Experimental Approaches for Biomolecule Interactions with Inorganic Surfaces. *J Biomed Mater Res A* **2013**, *101*, 1210-1222.
27. Muir, J. M. R.; Costa, D.; Idriss, H., DFT Computational Study of the RGD Peptide Interaction with the Rutile TiO_2 (110) Surface. *Surf Sci* **2014**, *624*, 8-14.
28. Wu, C. Y.; Skelton, A. A.; Chen, M. J.; Vlcek, L.; Cummings, P. T., Modeling the Interaction between Integrin-Binding Peptide (RGD) and Rutile Surface: The Effect of Cation Mediation on Asp Adsorption. *Langmuir* **2012**, *28*, 2799-2811.
29. Wu, C. Y.; Chen, M. J.; Skelton, A. A.; Cummings, P. T.; Zheng, T., Adsorption of Arginine-Glycine-Aspartate Tripeptide onto Negatively Charged Rutile (110) Mediated by Cations: The Effect of Surface Hydroxylation. *ACS Appl Mater Inter* **2013**, *5*, 2567-2579.
30. Song, D. P.; Chen, M. J.; Liang, Y. C.; Bai, Q. S.; Chen, J. X.; Zheng, X. F., Adsorption of Tripeptide RGD on Rutile TiO_2 Nanotopography Surface in Aqueous Solution. *Acta Biomater* **2010**, *6*, 684-694.
31. Zhang, H. P.; Lu, X.; Leng, Y.; Watari, F.; Weng, J.; Feng, B.; Qu, S. X., Effects of Aqueous Environment and Surface Defects on Arg-Gly-Asp Peptide Adsorption on Titanium Oxide Surfaces Investigated by Molecular Dynamics Simulation. *J Biomed Mater Res A* **2011**, *96A*, 466-476.
32. Meyers, S. R.; Hamilton, P. T.; Walsh, E. B.; Kenan, D. J.; Grinstaff, M. W., Endothelialization of Titanium Surfaces. *Adv Mater* **2007**, *19*, 2492-+.
33. Pierschbacher, M. D.; Ruoslahti, E., Cell Attachment Activity of Fibronectin Can Be Duplicated by Small Synthetic Fragments of the Molecule. *Nature* **1984**, *309*, 30-33.
34. Fang, Y.; Poulsen, N.; Dickerson, M. B.; Cai, Y.; Jones, S. E.; Naik, R. R.; Kroger, N.; Sandhage, K. H., Identification of Peptides Capable of Inducing the Formation of Titania but Not Silica Via a Subtractive Bacteriophage Display Approach. *J Mater Chem* **2008**, *18*, 3871-3875.
35. Sano, K. I.; Shiba, K., A Hexapeptide Motif That Electrostatically Binds to the Surface of Titanium. *J Am Chem Soc* **2003**, *125*, 14234-14235.
36. Yazici, H.; Fong, H.; Wilson, B.; Oren, E. E.; Amos, F. A.; Zhang, H.; Evans, J. S.; Snead, M. L.; Sarikaya, M.; Tamerler, C., Biological Response on a Titanium Implant-Grade Surface Functionalized with Modular Peptides. *Acta Biomater* **2013**, *9*, 5341-5352.
37. Puddu, V.; Slocik, J. M.; Naik, R. R.; Perry, C. C., Titania Binding Peptides as Templates in the Biomimetic Synthesis of Stable Titania Nanosols: Insight into the Role of Buffers in Peptide-Mediated Mineralization. *Langmuir* **2013**, *29*, 9464-9472.
38. Kyte, J.; Doolittle, R. F., A Simple Method for Displaying the Hydropathic Character of a Protein. *J Mol Biol* **1982**, *157*, 105-132.

39. Hayashi, T.; Sano, K. I.; Shiba, K.; Iwahori, K.; Yamashita, I.; Hara, M., Critical Amino Acid Residues for the Specific Binding of the Ti-Recognizing Recombinant Ferritin with Oxide Surfaces of Titanium and Silicon. *Langmuir* **2009**, *25*, 10901-10906.
40. Gertler, G.; Fleminger, G.; Rapaport, H., Characterizing the Adsorption of Peptides to TiO_2 in Aqueous Solutions by Liquid Chromatography. *Langmuir* **2010**, *26*, 6457-6463.
41. Fukuta, M.; Zheng, B.; Uenuma, M.; Okamoto, N.; Uraoka, Y.; Yamashita, I.; Watanabe, H., Controlled Charged Amino Acids of Ti-Binding Peptide for Surfactant-Free Selective Adsorption. *Colloid Surface B* **2014**, *118*, 25-30.
42. Chen, H. B.; Su, X. D.; Neoh, K. G.; Choe, W. S., Probing the Interaction between Peptides and Metal Oxides Using Point Mutants of a TiO_2-Binding Peptide. *Langmuir* **2008**, *24*, 6852-6857.
43. Chen, H. B.; Su, X. D.; Neoh, K. G.; Choe, W. S., QCM-D Analysis of Binding Mechanism of Phage Particles Displaying a Constrained Heptapeptide with Specific Affinity to SiO_2 and TiO_2. *Anal Chem* **2006**, *78*, 4872-4879.
44. Mirau, P. A.; Kotlarchyk, M.; Knecht, M.; Koerner, H.; Vaia, R.; Naik, R., Peptide Structure at Metal-Oxide and Metal Surfaces Probed by NMR. *Abstr Pap Am Chem S* **2012**, *244*.
45. Mirau, P. A.; Naik, R. R.; Gehring, P., Structure of Peptides on Metal Oxide Surfaces Probed by NMR. *J Am Chem Soc* **2011**, *133*, 18243-18248.
46. Wright, L. B.; Palafox-Hernandez, J. P.; Rodger, P. M.; Corni, S.; Walsh, T. R., Facet Selectivity in Gold Binding Peptides: Exploiting Interfacial Water Structure. *Chemical Science* **2015**, *6*, 5204-5214.
47. Friedrichs, W.; Koppen, S.; Langel, W., Titanium Binding Dodecapeptides and the Impact of Water Structure. *Surf Sci* **2013**, *617*, 42-52.
48. Agosta, L.; Zollo, G.; Arcangeli, C.; Buonocore, F.; Gala, F.; Celino, M., Water Driven Adsorption of Amino Acids on the (101) Anatase TiO_2 Surface: An Ab Initio Study. *Phys Chem Chem Phys* **2015**, *17*, 1556-1561.
49. Schneider, J.; Colombi Ciacchi, L., Specific Material Recognition by Small Peptides Mediated by the Interfacial Solvent Structure. *J Am Chem Soc* **2012**, *134*, 2407-2413.
50. Sano, K.; Ajima, K.; Iwahori, K.; Yudasaka, M.; Iijima, S.; Yamashita, I.; Shiba, K., Endowing a Ferritin-Like Cage Protein with High Affinity and Selectivity for Certain Inorganic Materials. *Small* **2005**, *1*, 826-832.
51. Puddu, V.; Perry, C. C., Peptide Adsorption on Silica Nanoparticles: Evidence of Hydrophobic Interactions. *ACS Nano* **2012**, *6*, 6356-6363.
52. Hughes, Z. E.; Walsh, T. R., What Makes a Good Graphene-Binding Peptide? Adsorption of Amino Acids and Peptides at Aqueous Graphene Interfaces. *J Mater Chem B* **2015**, *3*, 3211-3221.
53. Terakawa, T.; Kameda, T.; Takada, S., On Easy Implementation of a Variant of the Replica Exchange with Solute Tempering in Gromacs. *J Comput Chem* **2011**, *32*, 1228-1234.
54. Wright, L. B.; Walsh, T. R., Efficient Conformational Sampling of Peptides Adsorbed onto Inorganic Surfaces: Insights from a Quartz Binding Peptide. *Phys Chem Chem Phys* **2013**, *15*, 4715-4726.
55. Jonsson, C. M.; Jonsson, C. L.; Sverjensky, D. A.; Cleaves, H. J.; Hazen, R. M., Attachment of L-Glutamate to Rutile (Alpha-TiO_2): A Potentiometric, Adsorption, and Surface Complexation Study. *Langmuir* **2009**, *25*, 12127-12135.
56. Roddick-Lanzilotta, A. D.; Connor, P. A.; McQuillan, A. J., An in Situ Infrared Spectroscopic Study of the Adsorption of Lysine to TiO_2 from an Aqueous Solution. *Langmuir* **1998**, *14*, 6479-6484.
57. Skelton, A. A.; Walsh, T. R., Interaction of Liquid Water with the Rutile TiO_2 (110) Surface. *Mol Simulat* **2007**, *33*, 379-389.
58. Hook, F.; Rodahl, M.; Brzezinski, P.; Kasemo, B., Energy Dissipation Kinetics for Protein and Antibody-Antigen Adsorption under Shear Oscillation on a Quartz Crystal Microbalance. *Langmuir* **1998**, *14*, 729-734.
59. Sauerbrey, G., Verwendung Von Schwingquarzen Zur Wägung Dünner Schichten Und Zur Mikrowägung. *Zeitschrift für Physik* **1959**, *155*, 206-222.
60. Höök, F.; Kasemo, B.; Nylander, T.; Fant, C.; Sott, K.; Elwing, H. Variations in Coupled Water, Viscoelastic Properties, and Film Thickness of a Mefp-1 Protein Film During Adsorption and Cross-

Linking: A Quartz Crystal Microbalance with Dissipation Monitoring, Ellipsometry, and Surface Plasmon Resonance Study, *Anal. Chem.* **2001**, *73*, 5796–5804.
61. Fischer, H.; Polikarpov, I.; Craievich, A. F. Average Protein Density is a Molecular-Weight-Dependent Function, *Protein Sci.* **2004**, *13*, 2825–2828.
62. MacKerell, A. D.; Bashford, D.; Bellott, M.; Dunbrack, R. L.; Evanseck, J. D.; Field, M. J.; Fischer, S.; Gao, J.; Guo, H.; Ha, S.; Joseph-McCarthy, D.; Kuchnir, L.; Kuczera, K.; Lau, F. T. K.; Mattos, C.; Michnick, S.; Ngo, T.; Nguyen, D. T.; Prodhom, B.; Reiher, W. E.; Roux, B.; Schlenkrich, M.; Smith, J. C.; Stote, R.; Straub, J.; Watanabe, M.; Wiorkiewicz-Kuczera, J.; Yin, D.; Karplus, M., All-Atom Empirical Potential for Molecular Modeling and Dynamics Studies of Proteins. *J Phys Chem B* **1998**, *102*, 3586-3616.
63. Piana, S.; Lindorff-Larsen, K.; Shaw, D. E., How Robust Are Protein Folding Simulations with Respect to Force Field Parameterization? *Biophys J* **2011**, *100*, L47-L49.
64. Jorgensen, W. L.; Chandrasekhar, J.; Madura, J. D.; Impey, R. W.; Klein, M. L., Comparison of Simple Potential Functions for Simulating Liquid Water. *J Chem Phys* **1983**, *79*, 926-935.
65. Neria, E.; Fischer, S.; Karplus, M., Simulation of Activation Free Energies in Molecular Systems. *J Chem Phys* **1996**, *105*, 1902-1921.
66. Hess, B.; Kutzner, C.; van der Spoel, D.; Lindahl, E., Gromacs 4: Algorithms for Highly Efficient, Load-Balanced, and Scalable Molecular Simulation. *J Chem Theory Comput* **2008**, *4*, 435-447.
67. Predota, M.; Bandura, A. V.; Cummings, P. T.; Kubicki, J. D.; Wesolowski, D. J.; Chialvo, A. A.; Machesky, M. L., Electric Double Layer at the Rutile (110) Surface. 1. Structure of Surfaces and Interfacial Water from Molecular Dynamics by Use of Ab Initio Potentials. *J Phys Chem B* **2004**, *108*, 12049-12060.
68. Bonomi, M.; Branduardi, D.; Bussi, G.; Camilloni, C.; Provasi, D.; Raiteri, P.; Donadio, D.; Marinelli, F.; Pietrucci, F.; Broglia, R. A.; Parrinello, M., Plumed: A Portable Plugin for Free-Energy Calculations with Molecular Dynamics. *Comput Phys Commun* **2009**, *180*, 1961-1972.
69. Monti, S.; Li, C; Ågren, H.; Carravetta, V. Dropping a Droplet of Cysteine Molecules on a Rutile (110) Interface: Reactive versus Nonreactive Classical Molecular Dynamics Simulations, *J. Phys. Chem. C* **2015**, *119*, 6703-6712.
70. Wei, Y.; Latour, R. A. Determination of the Adsorption Free Energy for Peptide-Surface Interactions by SPR Spectroscopy. *Langmuir* **2008**, *24*, 6721-6729.
71. So, C. R.; Tamerler, C.; Sarikaya, M.; Adsorption, Diffusion and Self-Assembly of an Engineered Gold-Binding Peptide on Au(111) Investigated by Atomic Force Microscopy. *Angew. Chem., Int. Ed.* **2009**, *48*, 5174-5177.
72. Schlitter, J. Estimation of absolute and relative entropies of macromolecules using the covariance matrix. *Chem. Phys. Lett.* **1993**, *215*, 617-621.
73. Corni, S.; Hnilova,M.; Tamerler, C.; Sarikaya, M. Conformational Behavior of Genetically-Engineered Dodecapeptides as a Determinant of Binding Affinity for Gold. *J. Phys. Chem. C* **2013**, *117*, 16990-17003.

Figure and Table Captions

Table 1. Properties of peptide sequences Ti-1 and Ti-2 at pH 7. Hydropathy scores were generated from Kyte-Doolittle[57] indices.

Table 2. Free energies of adsorption, ΔG (kJ mol^{-1}) calculated from the QCM measurements of K_{eq}, for peptide sequences Ti-1 and Ti-2 adsorbed at the titania interface, both in water, and in salt solution (both at pH 7.4). The cross symbol indicates that no binding constant could be inferred.

Table 3. Analysis of peptide adsorption/desorption from QCM-D experiments leading to estimations on layer thickness using 10 μg/ml solutions (see Methods). Values quoted are derived from adsorption/desorption at equilibrium.

Figure 1. Exemplar QCM-D data on a) Ti-1 in 150 mM NaCl: gradual adsorption, precludes calculation of an equilibrium binding constant; b) Ti-2 in 0.15 M NaCl: adsorption at a range of concentrations, together with dissipation energy plot for the highest concentration studied; c) Langmuir plot of for Ti-2 using data from b) used for calculation of the binding free energy.

Figure 2. Exemplar QCM-D data for the binding of 10 μg/mL solutions of Ti-1 and Ti-2 to titania coated Ti sensors in, a) salt, and b) buffered water. The arrows signify when the sensor was washed with buffer alone.

Figure 4. Symmetrized final free energy profile of Ti-1 adsorbed at the aqueous titania interface. Dashed lines indicate the position of the titania surface (and its periodic image in the direction perpendicular to the surface).

Figure 3. Most likely adsorbed structures for Ti-1 and Ti-2, predicted from the REST-only simulations, also showing the averaged interfacial water density (blue). Molecular liquid water not shown for clarity. The black scale bars in each image show 1 nm.

Figure 5. Degree of residue-surface contact for peptides Ti-1 and Ti-2, generated from REST-only simulation data. Colored dots superimposed on the molecules indicate the degree of residue-surface direct contact. The tables use the same color scheme to indicate the amounts of direct and indirect (solvent mediated) surface contact, in addition to the total contact (direct+indirect).

Figure 6. Representative structures for Ti-1 and Ti-2 in solution, predicted from REST-only simulations.

Figure 7. Circular dichroism spectra of peptides Ti-1 (A) and Ti-2 (B) in water (0.5 mg/ml) and of peptides in the presence of the TiO_2 precursor. Reproduced from Ref. 37 with permission of the copyright owner.

	Sequence	Charge	Hydropathy
Ti-1	QPYLFATDSLIK	0	1.4
Ti-2	GHTHYHAVRTQT	1.3	-15.4

Table 1

Solvent	Ti-1	Ti-2
Water	-33.62 ± 0.43	-32.90 ± 0.88
Salt	×	-39.19 ± 0.11

Table 2

Experimental stage	**NaCl (0.15 M)**		**Water at pH 7.4**	
	Ti-1	**Ti-2**	**Ti-1**	**Ti-2**
Adsorption (ng/cm^2)	10.39	21.21	65.16	46.92
Desorption (ng/cm^2)	3.91	7.89	64.39	20.1
Estimated Peptide Density (g/mL)	1.54	1.57	1.54	1.57
Estimated Layer Thickness (Å)	6.75	13.50	42.31	29.86

Table 3

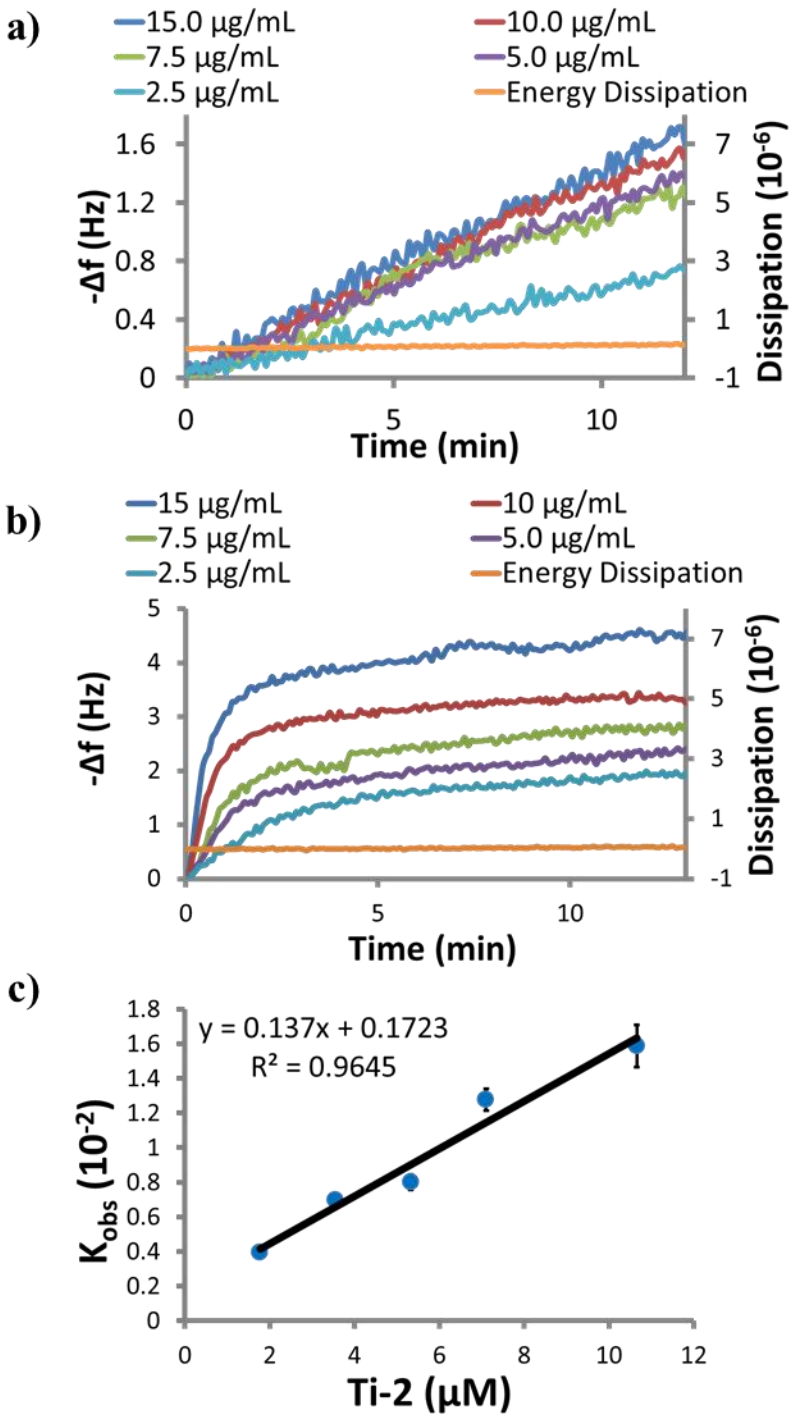
a)
15.0 µg/mL
10.0 µg/mL
7.5 µg/mL
5.0 µg/mL
2.5 µg/mL
Energy Dissipation
-Δf (Hz)
Dissipation (10-6)
Time (min)
b)
15 µg/mL
10 µg/mL
7.5 µg/mL
5.0 µg/mL
2.5 µg/mL
Energy Dissipation
-Δf (Hz)
Dissipation (10-6)
Time (min)
c)
y = 0.137x + 0.1723
R² = 0.9645
Kobs (10-2)
Ti-2 (µM)

Figure 1

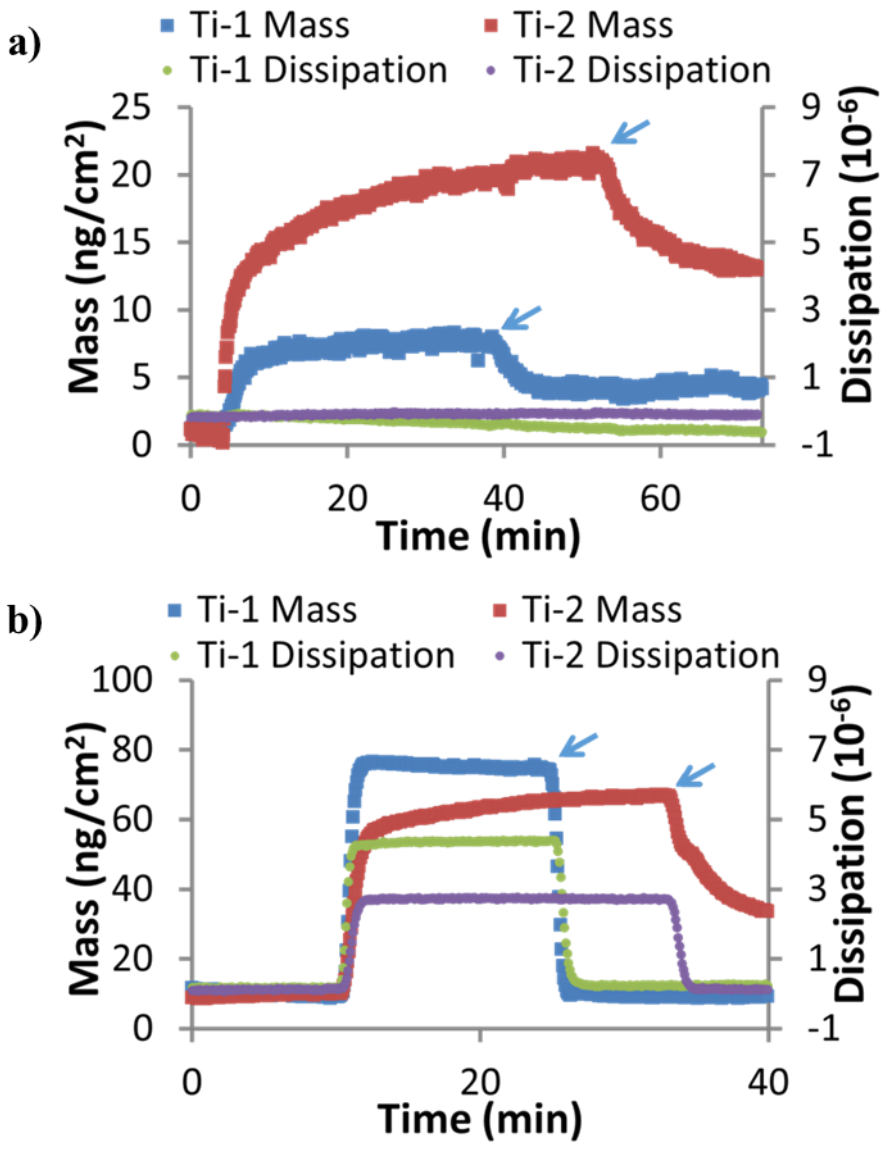
a)
Ti-1 Mass
Ti-2 Mass
Ti-1 Dissipation
Ti-2 Dissipation
Mass (ng/cm²)
Dissipation (10⁻⁶)
Time (min)
b)
Ti-1 Mass
Ti-2 Mass
Ti-1 Dissipation
Ti-2 Dissipation
Mass (ng/cm²)
Dissipation (10⁻⁶)
Time (min)

Figure 2

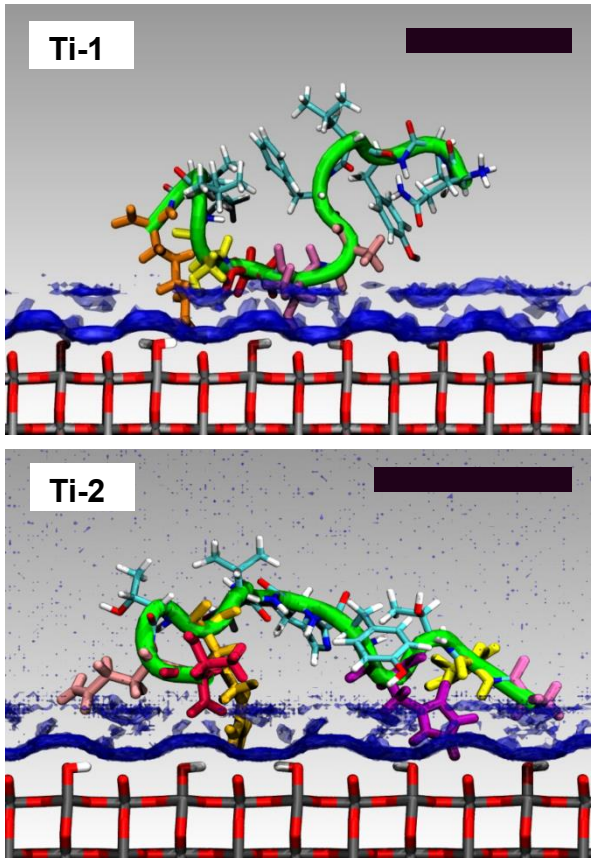

Figure 3

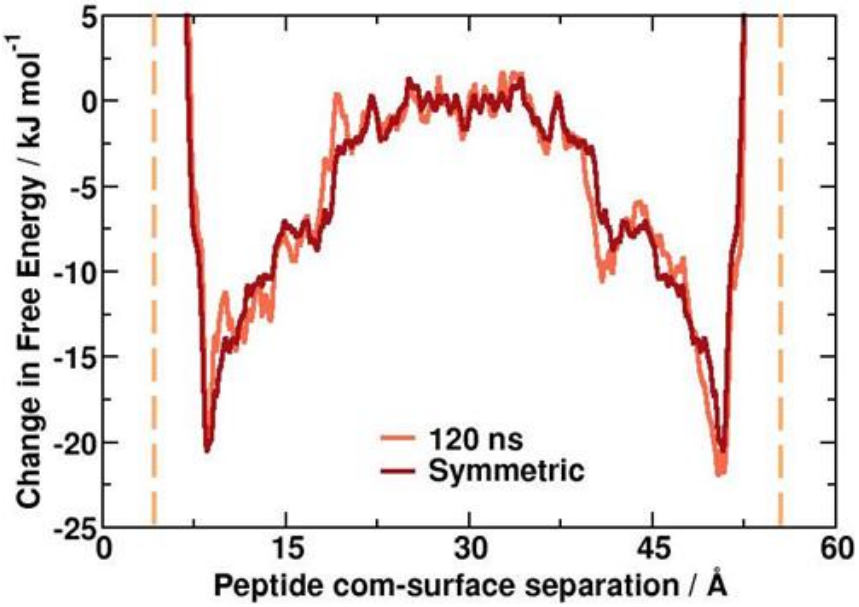
Change in Free Energy / kJ mol^{-1}
5
0
-5
-10
-15
-20
-25
0
15
30
45
60
Peptide com-surface separation / Å
120 ns
Symmetric

Figure 4

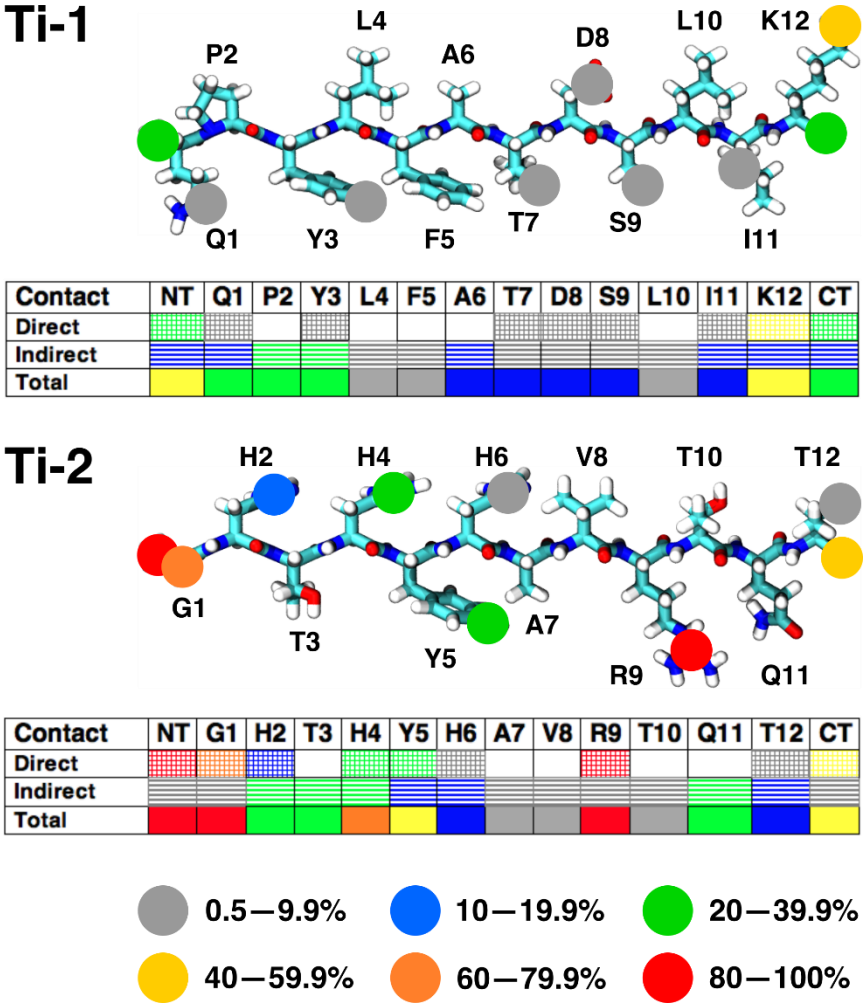
Ti-1
P2
L4
A6
D8
L10
K12
Q1
Y3
F5
T7
S9
I11
Contact
NT
Q1
P2
Y3
L4
F5
A6
T7
D8
S9
L10
I11
K12
CT
Direct
Indirect
Total
Ti-2
H2
H4
H6
V8
T10
T12
G1
T3
Y5
A7
R9
Q11
Contact
NT
G1
H2
T3
H4
Y5
H6
A7
V8
R9
T10
Q11
T12
CT
Direct
Indirect
Total
0.5—9.9%
10—19.9%
20—39.9%
40—59.9%
60—79.9%
80—100%

Figure 5

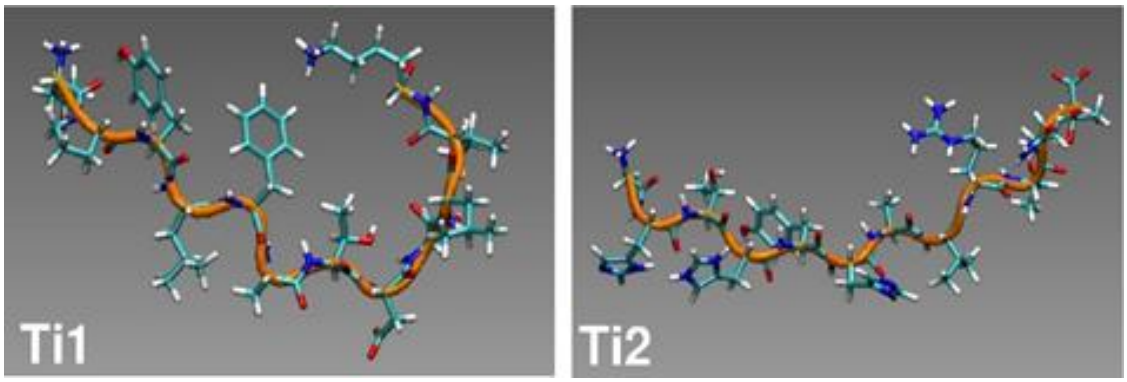

Figure 6

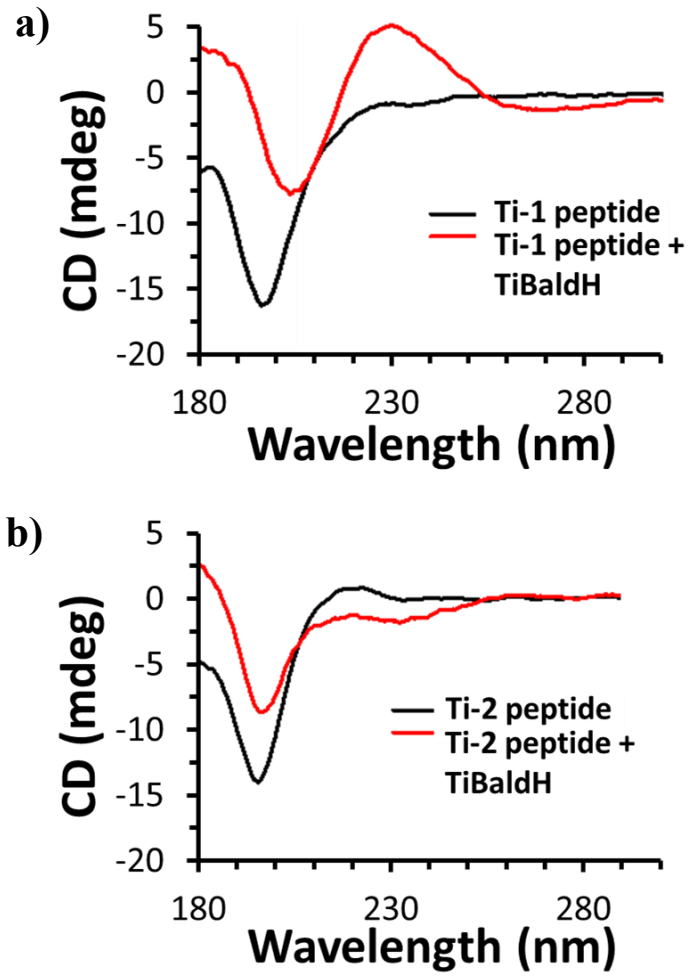
a)
5
0
-5
-10
-15
-20
CD (mdeg)
180
230
280
Wavelength (nm)
Ti-1 peptide
Ti-1 peptide +
TiBaldH
b)
5
0
-5
-10
-15
-20
CD (mdeg)
180
230
280
Wavelength (nm)
Ti-2 peptide
Ti-2 peptide +
TiBaldH

Figure 7

ToC Image:

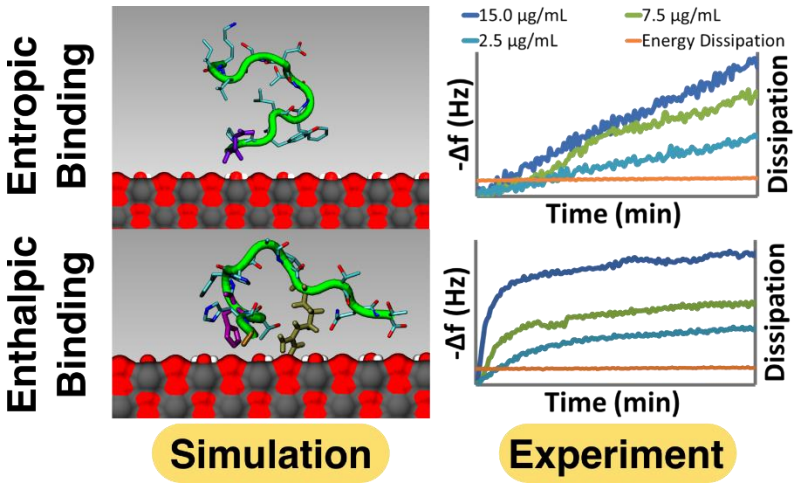
Entropic Binding
Enthalpic Binding
15.0 µg/mL
7.5 µg/mL
2.5 µg/mL
Energy Dissipation
-Δf (Hz)
Dissipation
Time (min)
-Δf (Hz)
Dissipation
Time (min)
Simulation
Experiment